Electronic Supplementary Material (ESI) for Nanoscale Advances.

Supplementary Information

Brain-like critical dynamics and long-range temporal correlations in percolating networks of silver nanoparticles and functionality preservation after integration of insulating matrix

Niko Carstens[a], Blessing Adejube[a], Thomas Strunskus[a], Franz Faupel[a], Simon Brown[b] and Alexander Vahl[a]*

[a] Institute for Materials Science, Chair for Multicomponent Materials, Faculty of Engineering, Kiel University, Kaiserstraße 2, D-24143 Kiel, Germany

[b] The MacDiarmid Institute for Advanced Materials and Nanotechnology, School of Physical and Chemical Sciences, Te Kura Matʻu, University of Canterbury, Private Bag 4800, Christchurch 8140, New Zealand

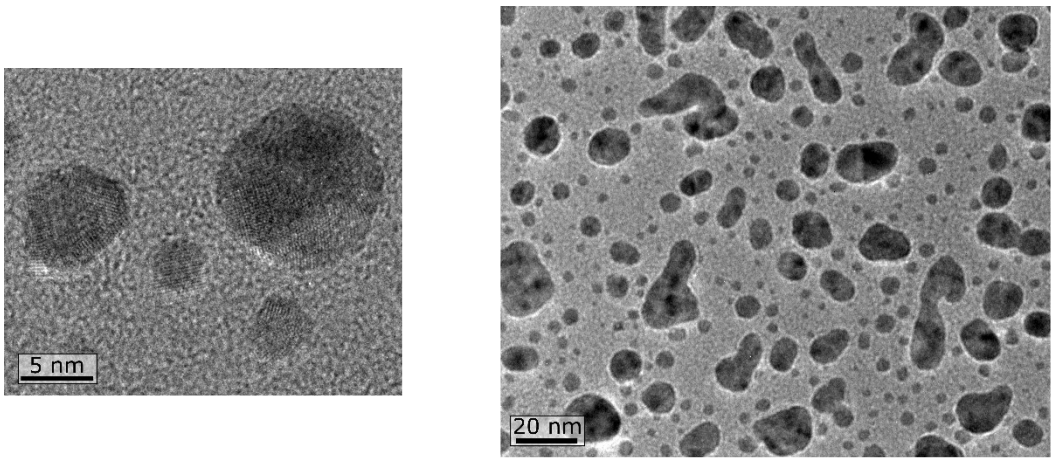

Figure S1. TEM images of Ag-NPs generated from GAS.

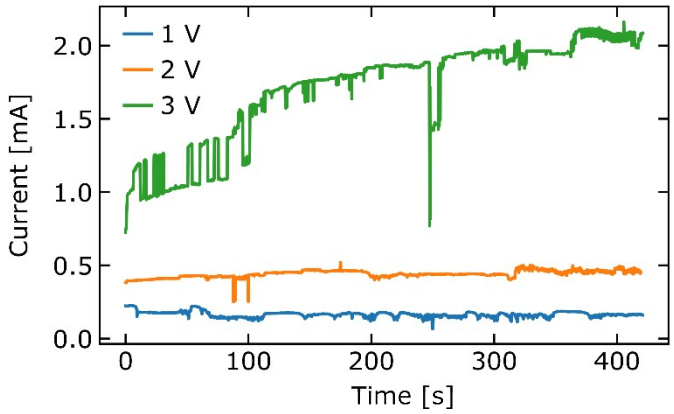

Figure S2. Current response of a percolating Ag-NP network with insulating matrix under different constant voltage inputs over time. A threshold behavior for switching activity can be observed, as typical for ECM-based systems.

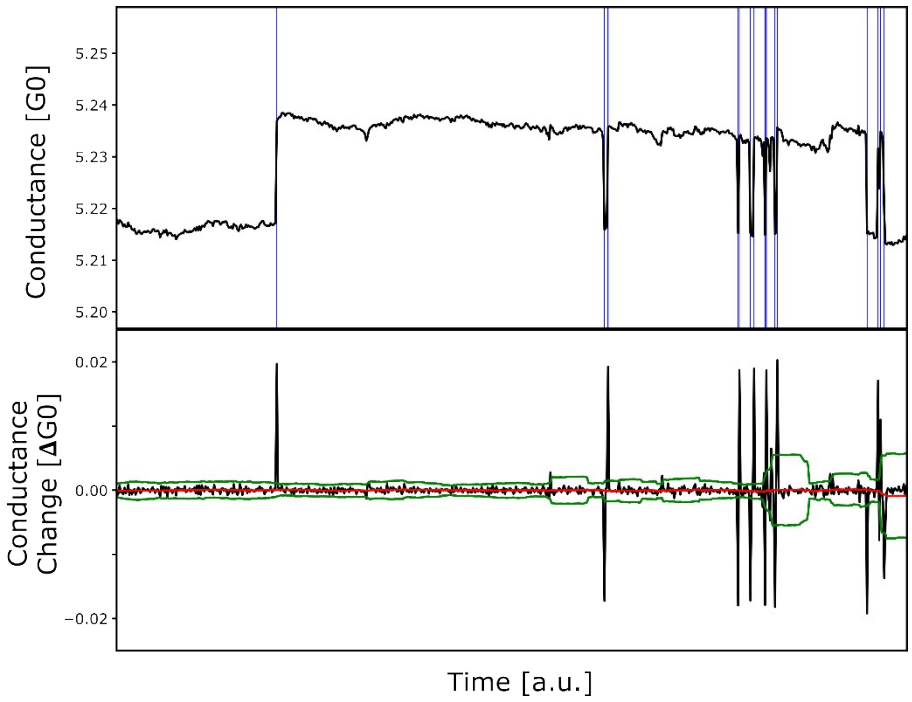

Figure S3. Illustration of transition event detection via a thresholding procedure for a sample without matrix. Top panel shows an exemplary time window of raw data in terms of network conductance versus time. Blue lines indicate transition events detected from the thresholding prodeduce. Thresholding was applied for the temporal sequence of conductance changes (lower panel). For each datapoint in the conductance change sequence, the mean level (red level) and threshold level (green level) were determined by calculating the mean and threefold standard deviation of the 30 past values in the sequence. When a conductance change exceeds the threshold level, it is designated as a network transition event. To account for a fundamental noise level, conductance change values lower than $0.01G_0$ were discarded. Conductance change values, which were detected as transition event, did not contribute to calculations of mean and threshold level.

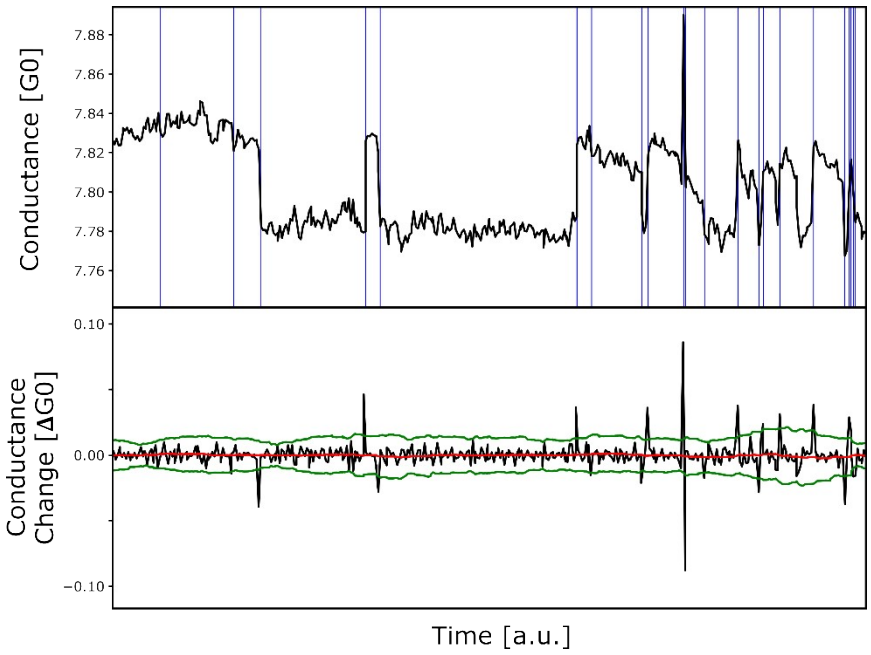

Figure S4. Same scheme as Figure S2, but with an exemplary time window of a sample with matrix.

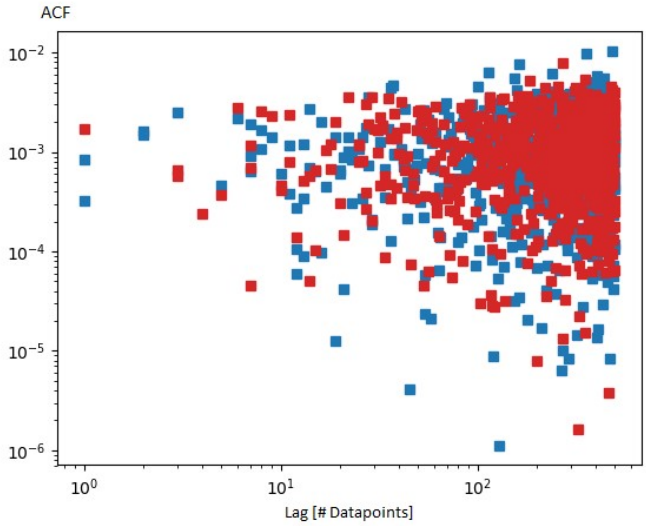

Figure S5. ACFs of all six samples (blue/red corresponds to samples without/with matrix) with shuffled time series of conductance changes. It can be seen that autocorrelation becomes destroyed upon randomizing.

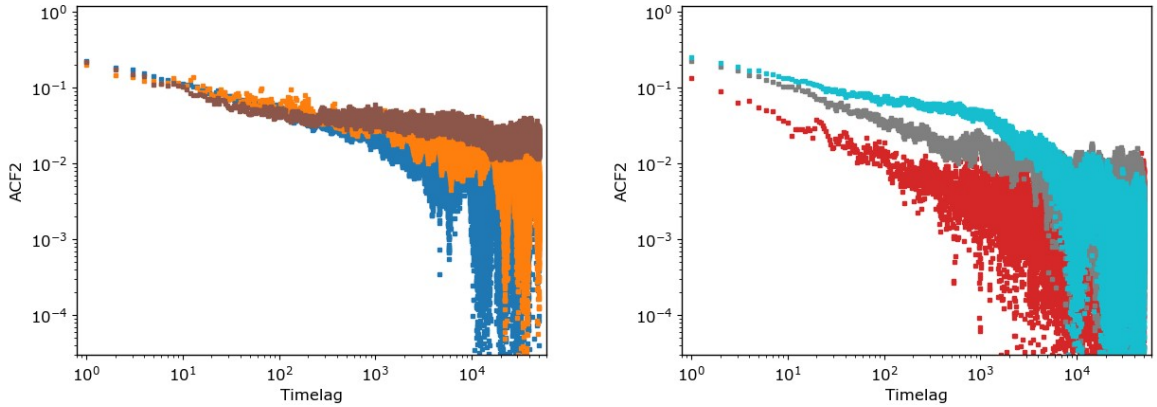

Figure S6. ACFs of samples without (left) and with (right) matrix shown to higher maximum lags. It can be seen, that long-range temporal correlations exists over several decades.

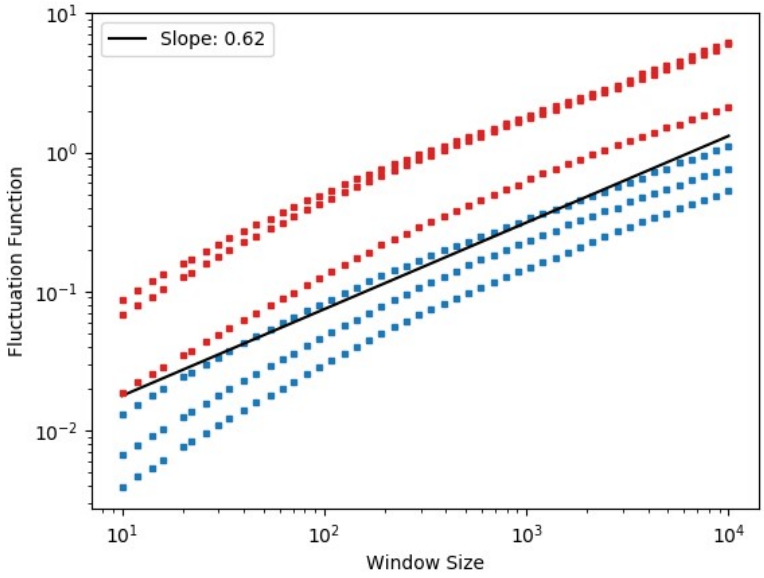

Figure S7. DFA of all six samples with shuffled time series. It can be seen that the slopes of the fluctuation functions are considerably decreased compared to the original data, indicating loss of temporal correlation. The Hurst exponents from the shuffled time series of conductance changes were determined as 0.62, 0.69 and 0.68 for samples without matrix and 0.68, 0.62 and 0.59 for samples with matrix. The black line shows the linear regression of fluctuation function versus window size for one sample without matrix for orientation.

Table S8. Observed event rates for all samples. Event rates were calculated for each sample as number of detected (i.e. thresholded) network transition events divided by total number current measurements over the whole long-term measurement. A higher event rate at equal measurement time decreases the probability of observing large interevent intervals, which was observed for samples with matrix (see Figure 4 bottom right). Although an unambiguous explanation for this observation is difficult, a possible hypothesis for the higher event rates of samples with matrix could be, that additional electron transport mechanisms are enabled by the presence of a matrix, which alters the activity of individual gaps. This is because in gaps without matrix, electron transport across a non-closed gap is only possible via direct tunneling, whereas in gaps with matrix nonlinear transport mechanisms like Fowler-Nordheim tunneling, Poole-Frenkel-emission or variable range or nearest neighbor hopping additionally contributes to the gap activity.

System	Sample	Datapoints of whole long-term measurement	Detected Network Transition Events	Event Rate [%]
Without Matrix	1	500000	28193	5.6
	2	500000	7558	1.5
	3	500000	12981	2.6
With Matrix	4	500000	33493	6.7
	5	500000	68043	13.6
	6	500000	82603	16.5

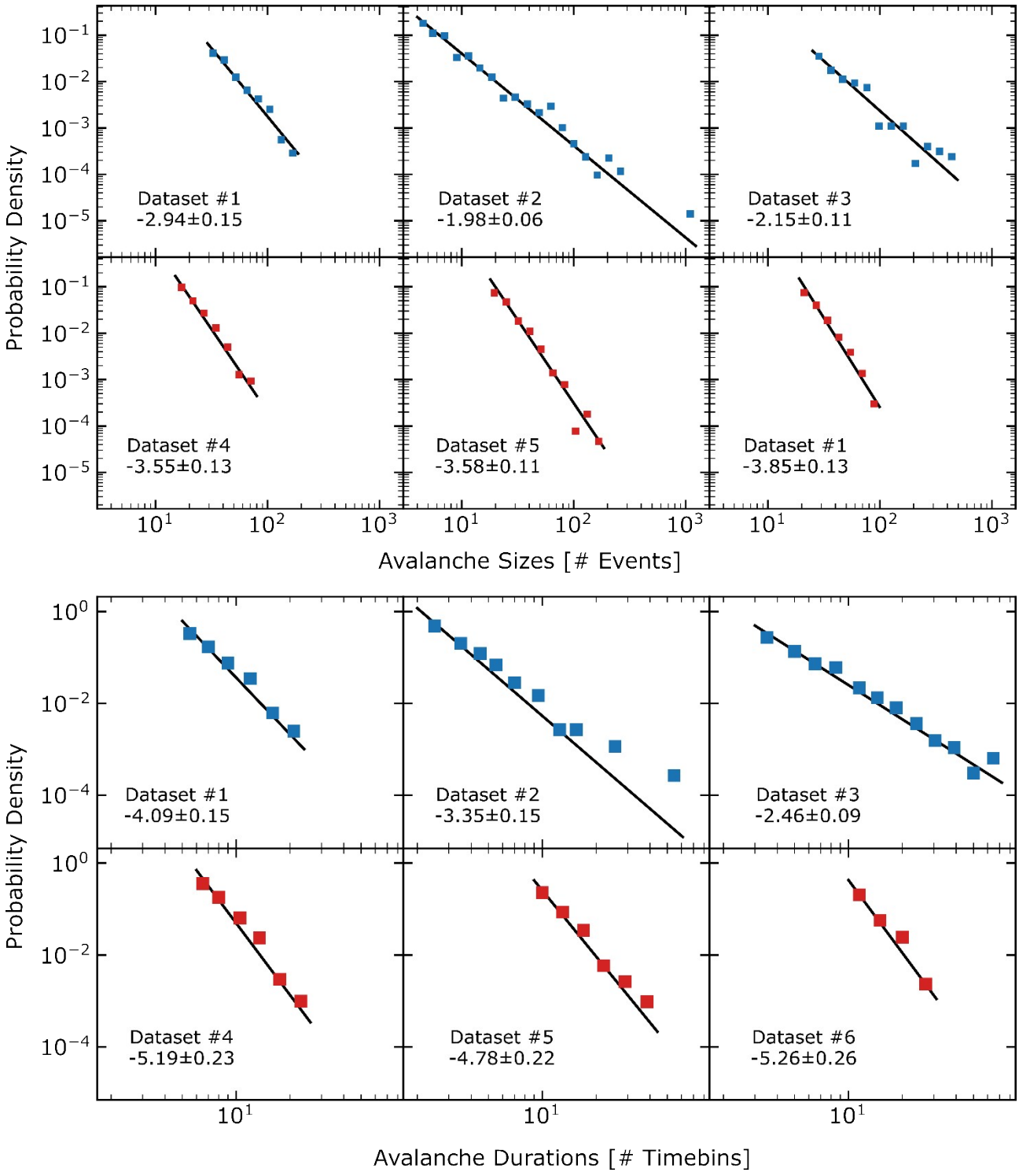

Figure S9. Fittings of avalanche size and duration distributions shown for each sample individually under application of a x_{min} value. From this, the power law exponents which were considered for the evaluation of the crackling noise relationship were extracted. Shown is the tail-part of the distribution above $x_{min.}$ The corresponding full empirical ranges are treated in Figure 6 in the main part.

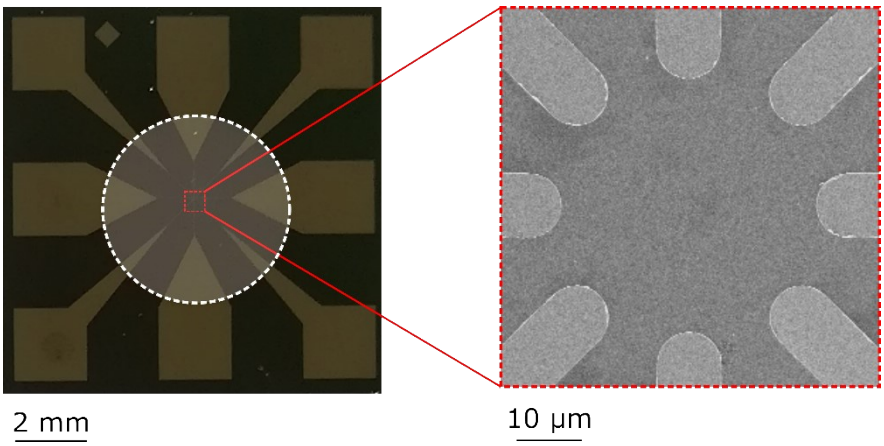

Figure S10. Optical image of a real sample (left) and an SEM image (right) showing the ends of electrodes. The white circle indicates the area of the NP film.

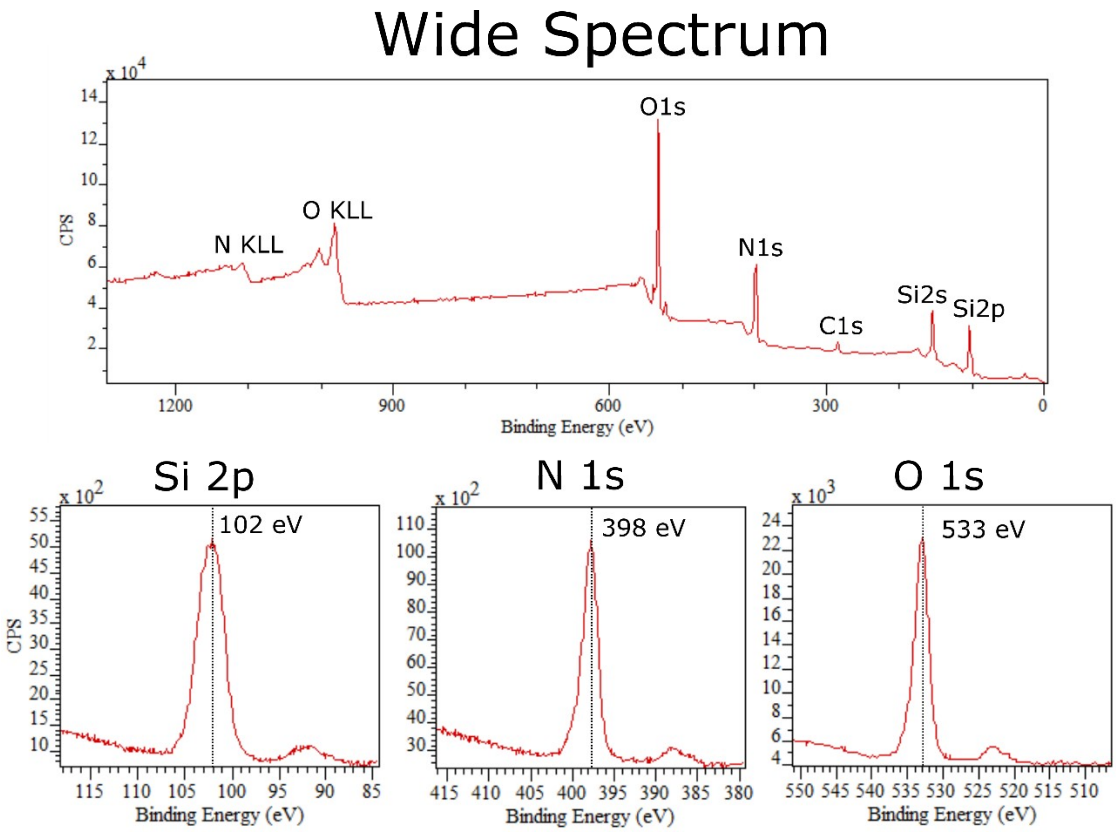

Figure S11. XPS analysis of matrix layer showing Si 2p, N 1s and O 1s peaks. The position of peaks suggests the existence of SiO_xN_y in the desposited matrix layer. The formation of an oxynitride can be attributed to an atmospheric oxidation of the matrix layer, which was deposited by a reactive gas mixture of Ar and N_2 from a Si target.

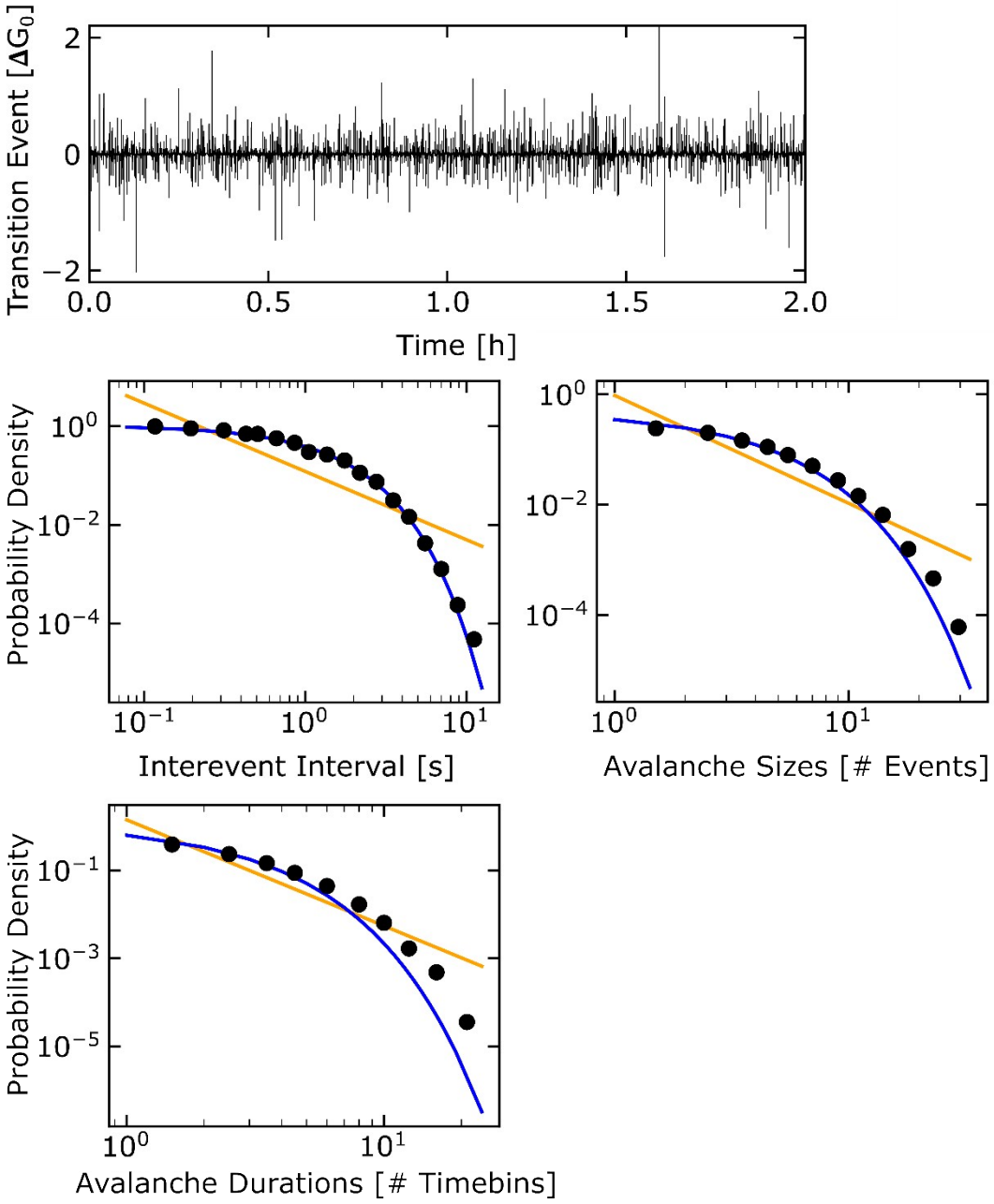

Figure S12. Power law analysis of IEIs and avalanches (following the same procedure as in the main text), but with randomized time series of network transition events. All in all, it can be seen that power law behavior becomes destroyed, as the distributions of dynamical characteristics now follow an exponential law (blue fit) instead of power law (orange fit).